machines

MDPI

Article

Parameter Self-Tuning of Servo Control Systems Based on Nonlinear Adaptive Whale Optimization Algorithm

Huarong Gu *, Xinyuan Wang and Xinyu Hu

College of Astronautics, Nanjing University of Aeronautics and Astronautics, Nanjing 211106, China; sx2315026@nuaa.edu.cn (X.W.); 1361174093@nuaa.edu.cn (X.H.)
* Correspondence: guhuarong@nuaa.edu.cn

Abstract

Parameter self-tuning of servo control systems is crucial for optimizing automation processes, especially in complex systems such as permanent magnet synchronous motors. In this paper, a nonlinear adaptive whale optimization algorithm (NAWOA) is proposed and applied to parameter self-tuning, which improves the traditional whale optimization algorithm (WOA) by nonlinearly adaptively adjusting two parameters during optimization to enhance fast convergence and global search capabilities. A servo control system with three parameters to be tuned is constructed using both simulation and physical methods. Simulation and experimental results show that the NAWOA outperforms the genetic algorithm, particle swarm optimization, and WOA in parameter self-tuning of the servo control system with lower error indicators and fast convergence speed. Although it still faces the challenge of initial condition dependency, the proposed NAWOA provides a powerful solution for real-time industrial applications.

Keywords: servo control system; permanent magnet synchronous motor; parameter self-tuning; search algorithm; whale optimization algorithm

1. Introduction

Parameter self-tuning is widely used in servo control systems [1–5]. Different combinations of controller parameters have a significant impact on the performance of servo control systems. For low-order control systems, the optimal parameter combination of different controller parameters can be artificially found by traversing the parameter combinations by trial and error. It is also possible to use empirical algorithms summarized by predecessors or derived from control principles, such as the Z-N (Ziegler Nichols) algorithm, to optimize the parameter combination. Such tuning methods are called model-based parameter self-tuning methods, whose core lies in the empirical summary of the trial-and-error process. However, they are no longer suitable for high-order control systems with more parameters and more external interferences, such as the permanent magnet synchronous motor (PMSM), whose size of the solution space grows exponentially as the number of parameters increases.

In recent years, with the rapid development of swarm intelligence algorithms [6–8], rule-based parameter self-tuning algorithms have gradually emerged and are favored by researchers. It treats the control system as a black box and achieves parameter tuning through iterative optimization based only on input, output, and search rules. These tuning methods have strong adaptability and versatility in different scenarios. Various swarm intelligence algorithms, such as the particle swarm optimization (PSO) algorithm [9–13]

Check for updates

Academic Editor: Dan Zhang

Received: 28 November 2025
Revised: 8 January 2026
Accepted: 18 February 2026
Published: 21 February 2026

Copyright: © 2026 by the authors. Licensee MDPI, Basel, Switzerland. This article is an open access article distributed under the terms and conditions of the Creative Commons Attribution (CC BY) license.

and the genetic algorithm (GA) [14–18], have been used for parameter self-tuning of servo control systems and have shown good performance. Nevertheless, they suffer from inherent drawbacks, such as large solution spaces, long search times, and a tendency to converge to local optima prematurely.

To address the issues above, a new rule-based method called the whale optimization algorithm (WOA) [19] has been proposed. WOA is a heuristic swarm intelligence search algorithm inspired by the feeding behavior of humpback whales. By simulating the whales' encircling prey, searching for prey and spiral bubble-net attacking mechanisms, this algorithm has demonstrated good performance in various fields [20–22]. However, WOA still faces some challenges, such as limited convergence accuracy, susceptibility to getting trapped in local optima, and strong dependence on the initial solution. Furthermore, when applying WOA to parameter self-tuning of servo control systems, the characteristics of the problem should be carefully considered, and appropriate improvements should be made to enhance the performance of the original algorithm. In this paper, the traditional WOA is improved by nonlinearly adaptively adjusting two parameters during optimization to enhance fast convergence and global search capabilities. The proposed nonlinear adaptive whale optimization algorithm is applied to the parameter self-tuning of a servo control system demonstrating superior performance.

2. Methods

2.1. Servo Control System

The servo control system under investigation is composed of three closed loops including current loop, speed loop and position loop, as shown in Figure 1. The input of the system is the position command and the output of the system is the three-phase stator winding current (i_A, i_B, i_C) with control information. In this paper, the parameters to be tuned of the servo control system include the proportional coefficient K_{pp} of the position P controller, the proportional coefficient K_{vp} and the integral time constant K_{vi} of the speed PI controller.

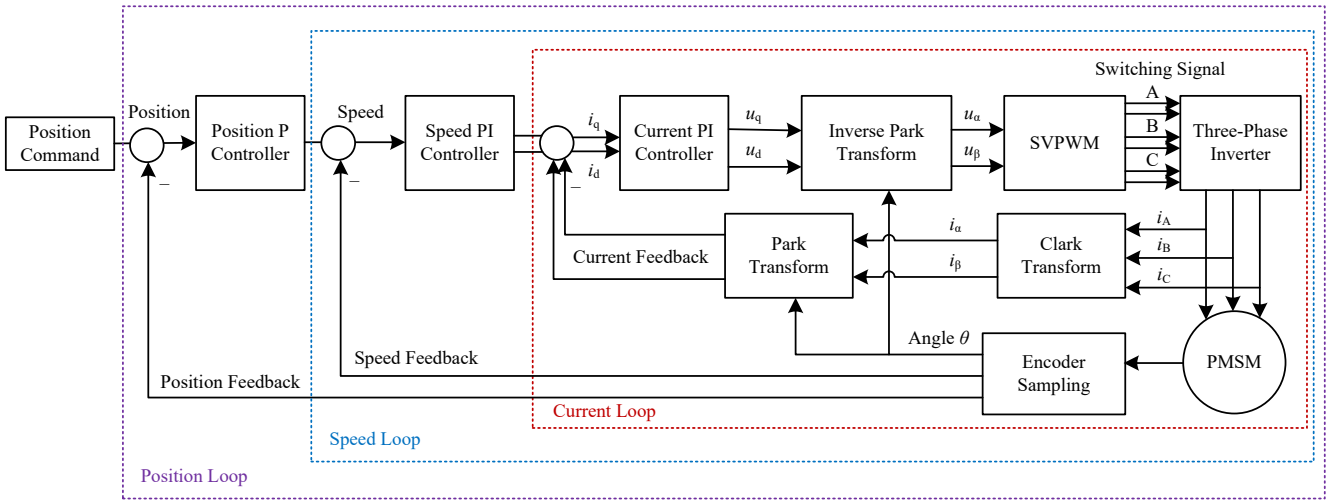


Figure 1. Block diagram of a servo control system.

The position error $e(t)$ can be obtained by subtracting the position feedback from the position command in Figure 1. The performance indices used in this paper are the time integrals of the position error, including integral time absolute error (ITAE), integral

absolute error (IAE), integral time square error (ITSE), and integral square error (ISE), which are defined as follows:

$$\text{ITAE} = \int_0^T t|e(t)|\mathrm{d}t, \tag{1}$$

$$\text{IAE} = \int_0^T |e(t)|\mathrm{d}t, \tag{2}$$

$$\text{ITSE} = \int_0^T t \cdot e^2(t)\mathrm{d}t, \tag{3}$$

$$\text{ISE} = \int_0^T e^2(t)\mathrm{d}t, \tag{4}$$

where t is the time variable, and T is the signal duration. Considering that these four performance indices have strong engineering practicality and the servo control system is a long-term running system, the error integrals can be used as performance indicators to effectively evaluate the degree of error accumulation of the system during long-term operation, thereby effectively improving the control accuracy and stability of the system.

2.2. Traditional Whale Optimization Algorithm

The optimal parameter combination of the servo control system can be found using the traditional whale optimization algorithm [19]. Assuming the whale population is N, the position vector $\boldsymbol{X}$ of a whale is treated as a solution of the optimization problem. In our case, $\boldsymbol{X} = (K_{\text{pp}}, K_{\text{vp}}, K_{\text{vi}})$. During optimization, the position of the ith whale at iteration g is denoted by $\boldsymbol{X}_i^g$, then its position at the next iteration is updated using one of three strategies:

(1) Encircling Prey Strategy

$$\boldsymbol{X}_i^{g+1} = \boldsymbol{X}_{\text{best}}^g - A \cdot \left| C \cdot \boldsymbol{X}_{\text{best}}^g - \boldsymbol{X}_i^g \right|, \tag{5}$$

where $\boldsymbol{X}_{\text{best}}^g$ is the position vector of the best solution obtained so far, A is a vector of random numbers uniformly distributed in $[-a, a]$ for each dimension, a is a convergence factor with an initial value of 2 and decreases linearly to 0 with the increase in iteration number, and C is a random number uniformly distributed in $[0, 2]$.

(2) Searching for Prey Strategy

$$\boldsymbol{X}_i^{g+1} = \boldsymbol{X}_{\text{rand}}^g - A \cdot \left| C \cdot \boldsymbol{X}_{\text{rand}}^g - \boldsymbol{X}_i^g \right|, \tag{6}$$

where $\boldsymbol{X}_{\text{rand}}^g$ is a random position vector in the solution space selected from the available whales.

(3) Spiral Bubble-Net Attacking Strategy

$$\boldsymbol{X}_i^{g+1} = \left| \boldsymbol{X}_{\text{best}}^g - \boldsymbol{X}_i^g \right| \cdot \exp(bl) \cdot \cos(2\pi l) + \boldsymbol{X}_{\text{best}}^g, \tag{7}$$

where b is a constant for defining the shape of the logarithmic spiral, and l is a random number in $[-1, 1]$.

In traditional WOA, the probability of using the third strategy is 50%. In mathematical terms, choosing a random number p in $[0, 1]$ and a constant $P_L = 0.5$, if $p \geq P_L$, the position is updated using Equation (7). If $p < P_L$ and $|A| < 1$, the position is updated using Equation (5). If $p < P_L$ and $|A| \geq 1$, the position is updated using Equation (6).

2.3. Nonlinear Adaptive Whale Optimization Algorithm

Since the encircling prey strategy is a key factor in the convergence of WOA [23], the probability of using the first strategy should be increased in the early stages of the optimization process to accelerate convergence. Furthermore, the searching for prey strategy is crucial for the global search capability of WOA, and the probability of using the second strategy should also be increased. Therefore, we proposed a nonlinear adaptive whale optimization algorithm (NAWOA), with changes compared to WOA as follows:

- P_L varies with iteration g:

$$P_L(g) = \frac{1}{1+\exp\left[-\left(\frac{G}{g}-1\right)\right]} - P_c, \tag{8}$$

where $P_c \in (0, 0.5)$, and G is the maximum number of iterations.

The smaller the value of P_c, the higher the probability of encircling prey and searching for prey. However, the value of P_c should not be too small, to ensure a reasonably high probability of entering spiral bubble-net attacking in the later stages of iteration. Thus, we choose P_c = 0.1. Taking $G = 10$ as an example, $P_L \in [0.4, 0.9)$ can be calculated as shown in Figure 2. It can be seen that P_L is greater than 0.5 in the early stages of iterations ensuring a higher probability of encircling prey and searching for prey, which is beneficial for fast convergence and global search. In the later stages of iterations, P_L is less than 0.5 leading to a higher probability of spiral bubble-net attacking that might result in a better local solution.

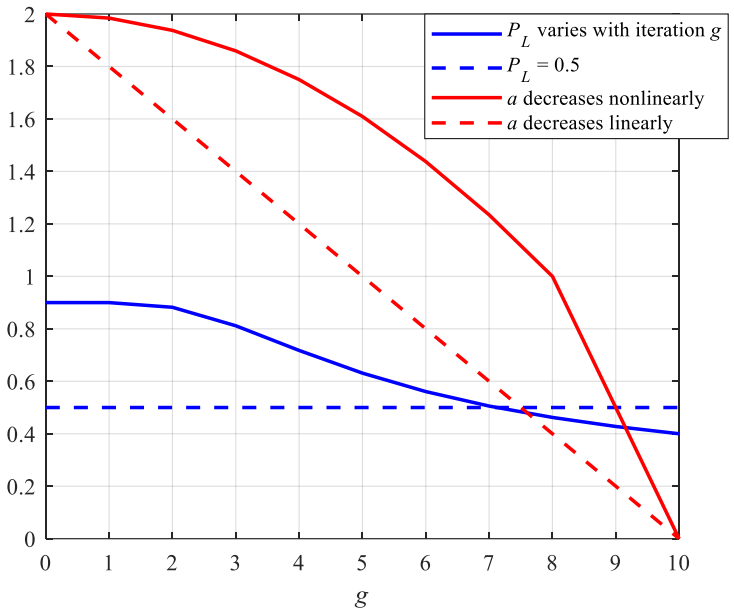


Figure 2. Changes in parameters involved in the optimization algorithm with iteration number.

- a decreases nonlinearly with iteration g:

$$a(g) = \begin{cases} 2 - \frac{g^2}{m^2 G^2}, & \text{if } 0 \le g \le mG; \\ \frac{1}{1-m}\left(1 - \frac{g}{G}\right), & \text{if } mG < g \le G; \end{cases} \tag{9}$$

where $m \in (0.5, 1)$ is a constant determining the segmentation point of the piecewise function.

The larger the value of m, the greater the probability of searching for prey. However, the value of m should not be too large, to avoid losing the optimal solution in the later stages

of iteration. Therefore, we choose m = 0.8. Taking $G = 10$ as an example, the descending curve of $a(g)$ is shown in Figure 2. It can be seen that a is greater than 1 for most iterations, which gives a certain probability of searching for prey that is beneficial for global search.

We applied the proposed nonlinear adaptive whale optimization algorithm to the parameter self-tuning of the aforementioned servo control system. The flowchart of NAWOA is shown in Figure 3.

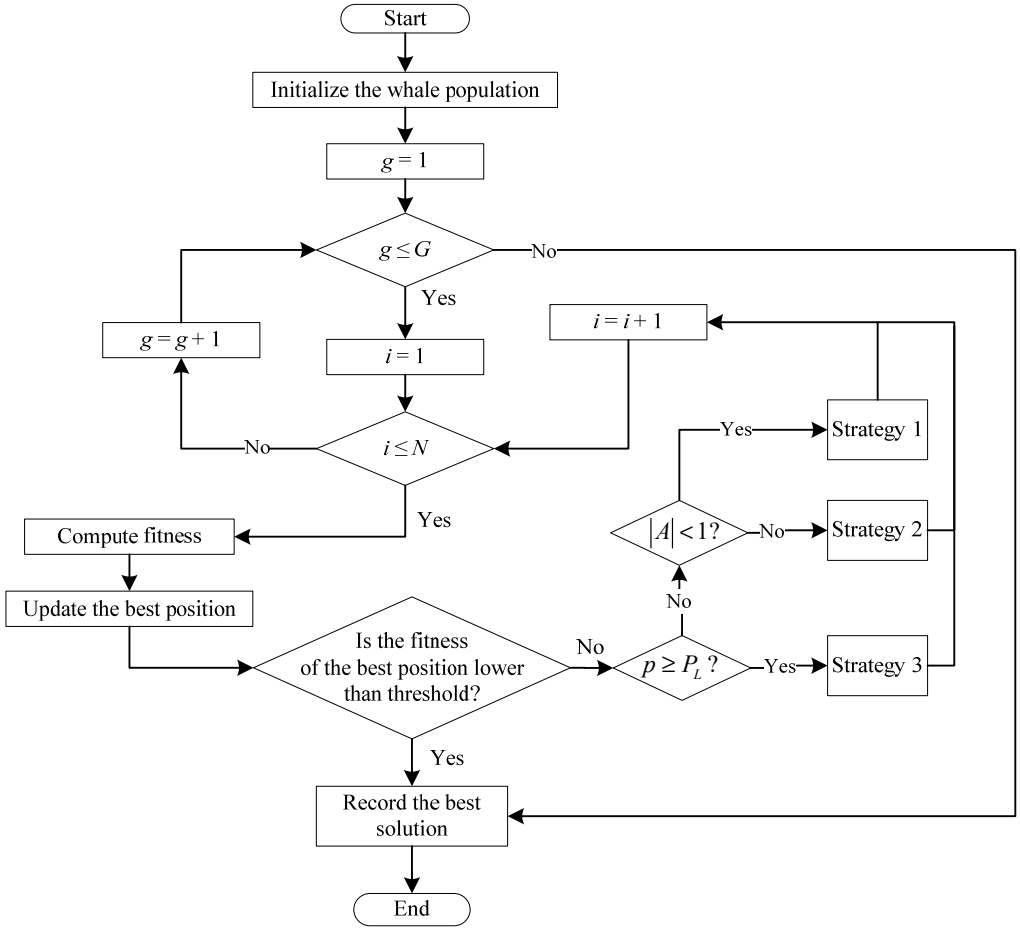


Figure 3. Flowchart of NAWOA.

3. Results and Discussion

3.1. Simulation Results and Discussion

Simulations were conducted on MATLAB R2022a. The code for optimization algorithms was written in MATLAB, while Simulink was used for simulation modeling of the servo control system. The Simulink model includes modules for the position P controller, speed PI controller, inverse Park transform, space vector pulse width modulation (SVPWM), three-phase inverter, PMSM, Clark transform, Park transform, signal input, error calculation, and so on. The error calculation modules consist of ITAE, IAE, ITSE, and ISE.

Data exchange between optimization algorithms and the simulation model occurs via the default workspace of MATLAB. The simulation model calculates the fitness value by integrating position error over the instruction cycle and feeds it back to the workspace through the simout variable. Figure 4 shows the timing diagram of data exchange between an optimization algorithm and a simulation model when the algorithm performs parameter self-tuning of a servo control system.

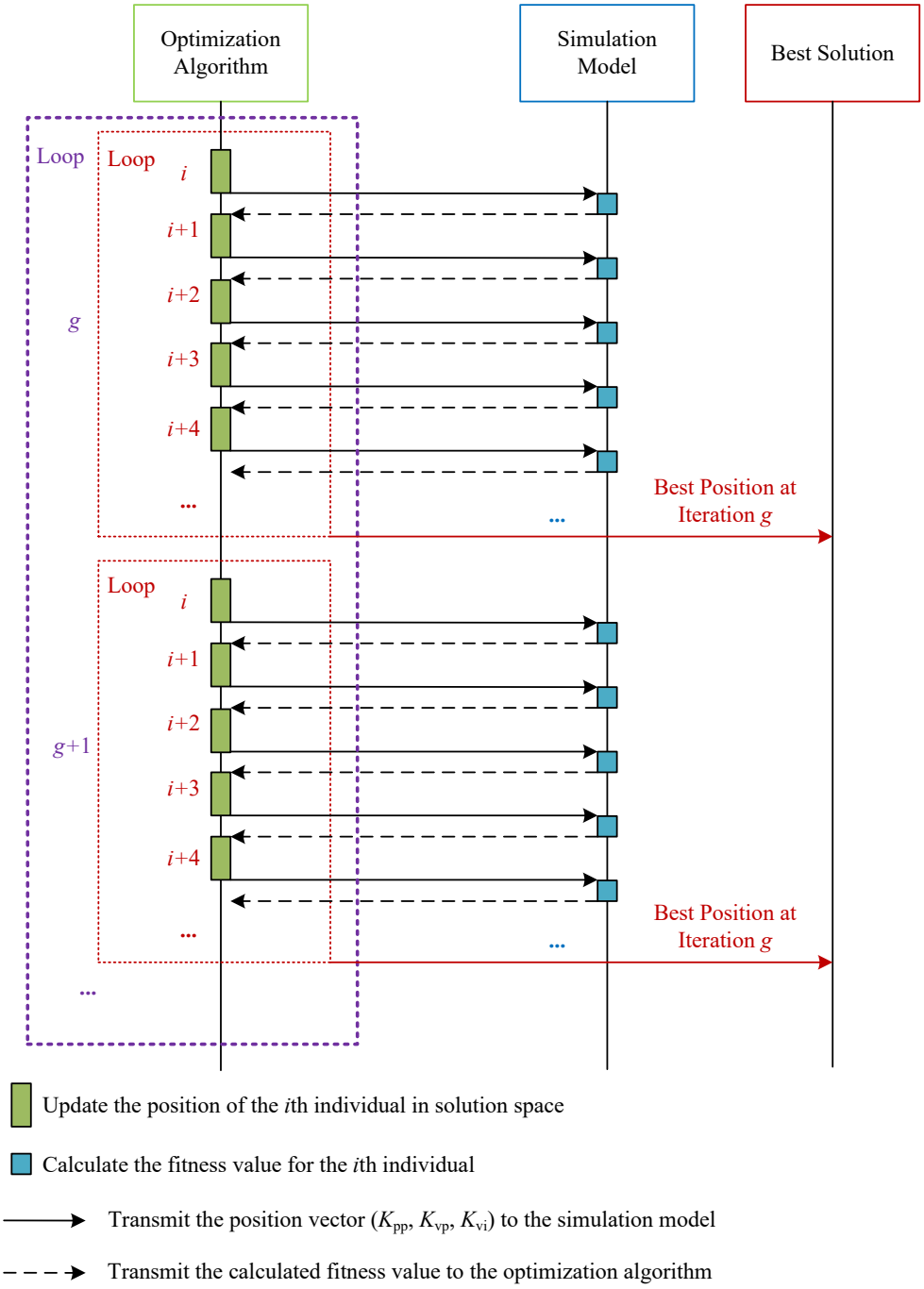


Figure 4. Timing diagram of data exchange for an optimization algorithm.

During simulation, we employed the PSO, GA, WOA, and NAWOA for parameter self-tuning of the servo control system. The PSO algorithm has a maximum value of inertia factor of 0.5, a minimum value of inertia factor of 0.08, an individual historical learning factor of 2, and a global learning factor of 4. The GA has a mutation probability of 0.7 and a crossover probability of 0.5. For the NAWOA, $P_c = 0.1$ and $m = 0.8$. For all four algorithms, the population size N is 50, the maximum number of iterations G is 10, and the search range for each parameter is [0, 50,000]. To avoid the influence of initial conditions, all of the above algorithms were run multiple times, and the best result from each was selected for analysis.

From Figures 5–8, it can be seen that the GA generally exhibits poor self-tuning performance with higher error indices, while the NAWOA outperforms the other three

algorithms in parameter self-tuning across all four performance indices including ITAE, IAE, ITSE, and ISE. Since ITAE can effectively suppress persistent minor errors and minimize oscillations in the system's transient response, it is used as the only performance index and fitness value for the system subsequently.

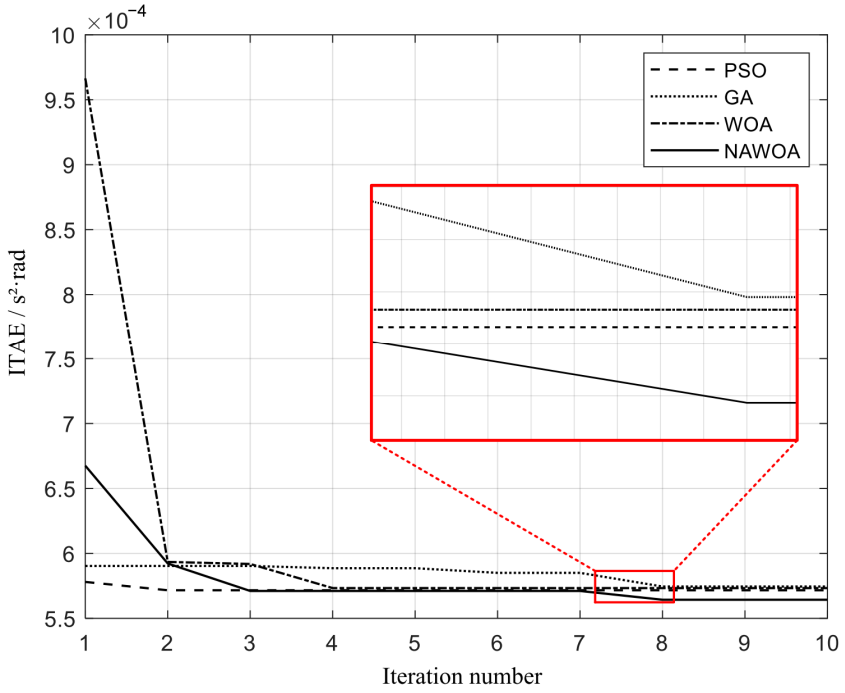


Figure 5. Simulation ITAE decline curve with iteration number.

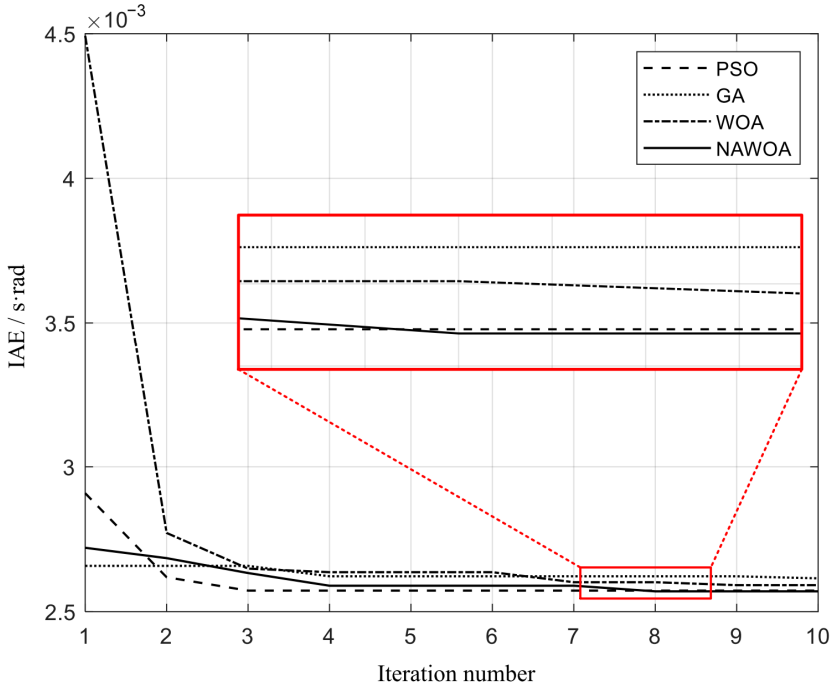


Figure 6. Simulation IAE decline curve with iteration number.

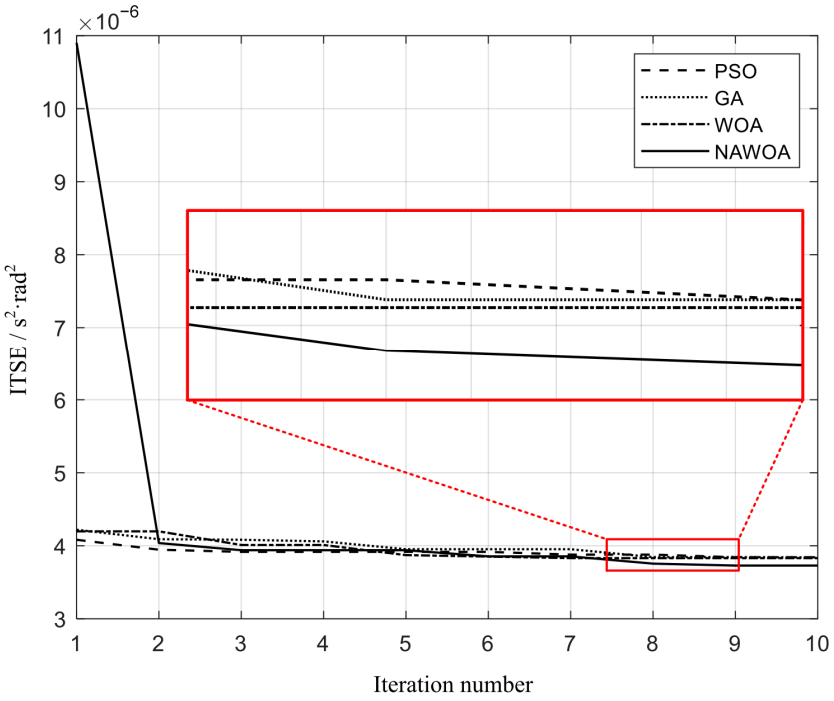


Figure 7. Simulation ITSE decline curve with iteration number.

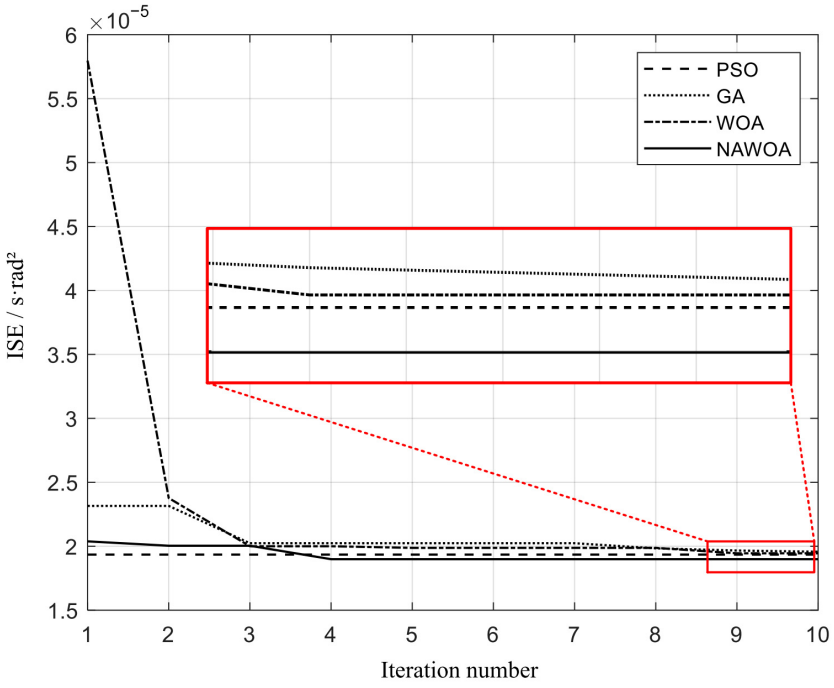


Figure 8. Simulation ISE decline curve with iteration number.

Figure 9 shows the characteristics of the four optimization algorithms in the solution space. The GA exhibits the most scattered distribution. PSO shows a denser pattern than GA. The distributions of the WOA and NAWOA are relatively concentrated, clustering around the optimal solution, i.e., the green regions in the scatter plot.

Further analysis of Figure 9 and characteristics of each algorithm reveals that the GA generates strong randomness through crossover and mutation, resulting in significant differences and low similarity between consecutive iterations. This mechanism expands the search scope, enhancing global search capabilities but reducing the accuracy of local searches. Consequently, when the population size is small or the number of iterations

is limited, the GA performs worse than the PSO, WOA, and NAWOA. In contrast, the PSO, WOA, and NAWOA update positions based on the previous iteration with weaker randomness. This strengthens the memory between iterations, reduces positional shifts, and focuses the search on local regions, thereby improving local search capabilities. Upon convergence, the PSO, WOA, and NAWOA typically yield better optimal solutions than the GA.

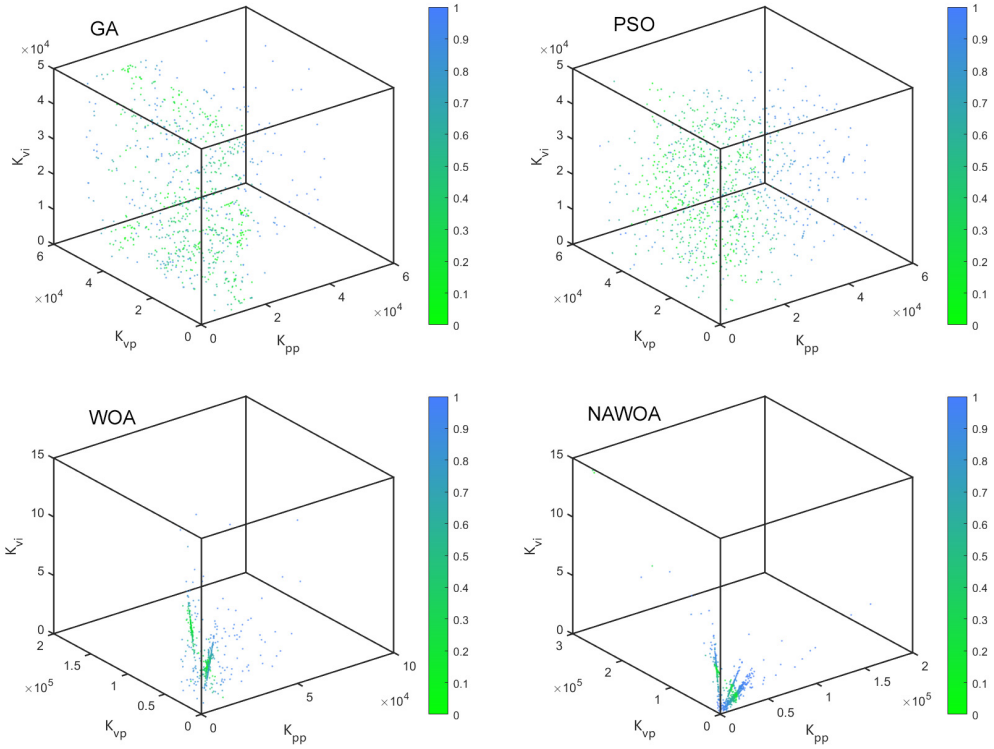


Figure 9. Scatter plot of the positions of the solutions of the four algorithms in solution space. The bluer the color in the legend, the larger the ITAE value and the worse the control performance; the greener the color, the smaller the ITAE value and the better the control performance.

To deeply investigate the search behavior and performance of NAWOA in parameter self-tuning of servo control systems, we enlarged the 3D scatter plot of NAWOA in Figure 9 and projected it into left, front, and top views, as shown in Figure 10. The red rectangles in the front and top views indicate that the optimal solutions found by the NAWOA are distributed around K_{pp} = 20,000 and are independent of K_{vp} and K_{vi}. By observing the red rectangles in the left view, although no obvious law was found in the distribution of optimal solutions, the scattered points exhibited a linear distribution, which is consistent with the encircling prey strategy of NAWOA. It can also be observed that the clustering of scattered points is denser around the core of the linear distribution, while the distribution of scattered points is more dispersed at both ends of the linear distribution. The overall view of the 3D scatter plot provides a more intuitive way to see the actual path that the NAWOA searches throughout the solution space. It can be observed that the scattered points distributed along several straight lines eventually lead to the red-boxed regions containing the optimal solutions. Therefore, the proposed NAWOA can still converge stably in a solution space with a very large search size and weak constraints in servo control system applications.

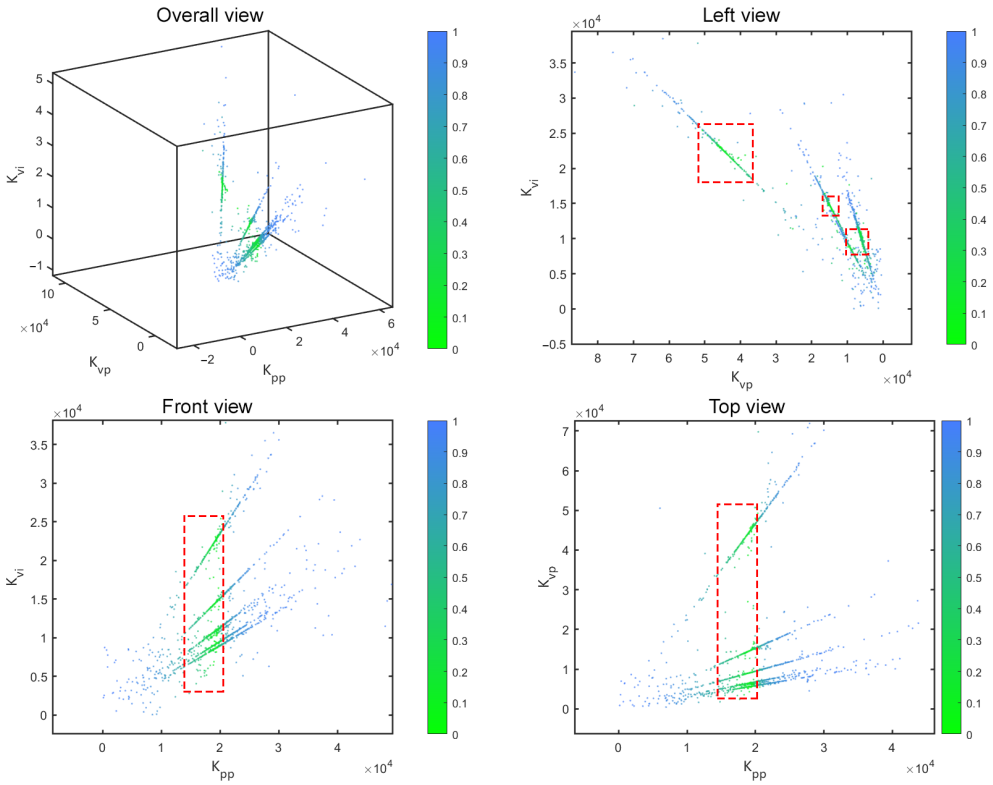


Figure 10. 3D scatter plot of the positions of the solutions of NAWOA in solution space and its three projection views. The red dashed squares indicate better solutions.

3.2. Experimental Results and Discussion

The experimental servo control system is mainly composed of a PMSM, a servo driver, and a computer, as shown in Figure 11. Parameter self-tuning algorithms are written in the debugging software on the computer. Parameters are updated in real time, and the corresponding firmware program is written into the servo driver to realize path planning of the input signal, cycle control, calculation of ITAE, and data transmission. PMSM parameters used in the experiment are listed in Table 1. Other parameters are the same as those in simulation.

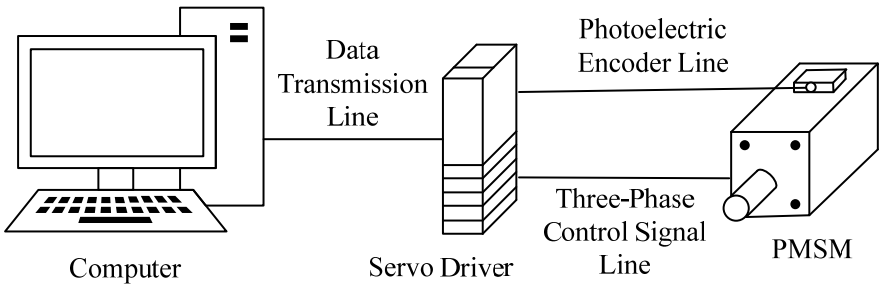


Figure 11. Experimental servo control system.

Experimental results are shown in Figure 12. It is evident that the NAWOA performs best, the GA performs the worst, and the PSO and WOAs perform similarly, which aligns closely with simulation results. The improved NAWOA, by adjusting the algorithm's decision probability P_L and structural parameter A, adaptively optimizes the probability of entering the three strategies during iteration. This improvement significantly enhances NAWOA's ability to escape local optima and compensates for the weak global search capability of WOA due to its spiral search strategy. The improved NAWOA achieves a

convergence speed close to that of WOA, and both outperform the GA and PSO in terms of convergence speed.

Table 1. Parameters of the permanent magnet synchronous motor.

Name	Unit	Value
Rated torque	Nm	1.27
Rated voltage	V	220
Rated speed	rpm	3000
Rated current	A	2.77
Stator resistance	Ω	3.23
Q-axis inductance	mH	4.597
D-axis inductance	mH	3.562
Flux linkage	Wb	0.049
Moment of inertia	10^{-4} kg/m^2	0.461
Number of poles	unitless	5

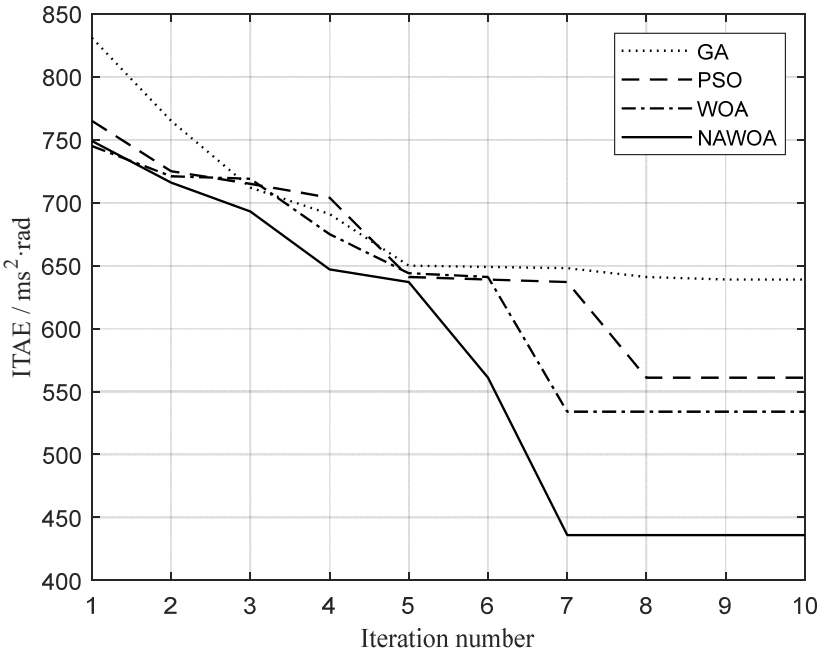


Figure 12. Experimental ITAE decline curve with iteration number when N = 50.

When the population size N is increased from 50 to 100, around the 5th iteration, as shown in Figure 13, the PSO, WOA, and NAWOA exhibit a notable drop in their ITAE curves, reflecting strong abilities to escape local optima. The GA shows a similar drop near the 8th iteration but lags in final tuning results and convergence speed. NAWOA's nonlinear adaptive improvements increase the likelihood of entering encircling prey and searching for prey strategies, boosting both convergence speed and global search capability.

Compared to Figure 12, increasing the population size with a fixed number of iterations reduced the final ITAE value, indicating better tuning performance. A larger population enhances the chance of finding superior solutions but increases the search scale and time cost. In our experiments, each search took approximately 1–2 s. A complete parameter self-tuning experiment with 500 searches took about 10 min. Thus, in practical tuning, the search scale should be tailored to balance performance needs and time constraints.

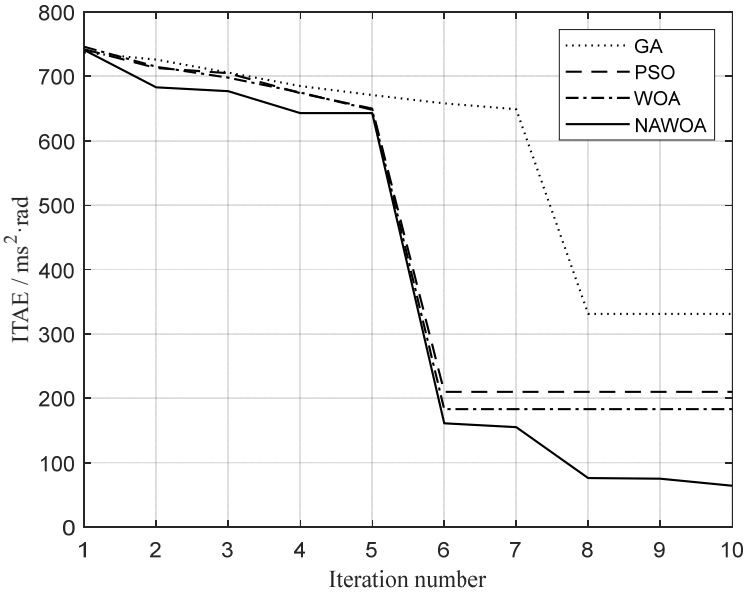


Figure 13. Experimental ITAE decline curve with iteration number when N = 100.

4. Conclusions

This paper presents a nonlinear adaptive whale optimization algorithm (NAWOA) for the parameter self-tuning of servo control systems. The decision probability P_L and the structural parameter A of the traditional whale optimization algorithm are nonlinearly adaptively adjusted to accelerate convergence and enhance global search capability. Simulations and experiments are carried out to verify the feasibility of the NAWOA in parameter self-tuning. Results show that the NAWOA outperforms the WOA and is significantly better than the GA and PSO. Applying the proposed NAWOA method to parameter self-tuning is expected to improve the performance of servo control systems. Future research could further investigate how to eliminate the influence of initial conditions on the NAWOA.

Author Contributions: Conceptualization, H.G. and X.H.; methodology, H.G. and X.H.; software, X.H.; validation, H.G., X.W. and X.H.; formal analysis, X.W.; investigation, X.H.; resources, H.G.; data curation, X.H.; writing—original draft preparation, X.W. and X.H.; writing—review and editing, H.G., X.W. and X.H.; visualization, X.H.; supervision, H.G.; project administration, H.G.; funding acquisition, H.G. All authors have read and agreed to the published version of the manuscript.

Funding: This research was funded by the National Key Research and Development Program of China, grant number 2022YFF0705500.

Data Availability Statement: The data presented in this study are available upon request from the corresponding author.

Acknowledgments: The authors would like to thank Peitian Robotics Technology Co., Ltd. for its support and help.

Conflicts of Interest: The authors declare no conflicts of interest.

References

1. Azahar, M.I.P.; Irawan, A.; Ismail, R.M.T.R. Self-tuning hybrid fuzzy sliding surface control for pneumatic servo system positioning. *Control. Eng. Pract.* **2021**, *113*, 104838. [CrossRef]
2. Wei, Y.; Wei, Y.J.; Sun, Y.N.; Qi, H.H.; Li, M.Y. An Advanced Angular Velocity Error Prediction Horizon Self-Tuning Nonlinear Model Predictive Speed Control Strategy for PMSM System. *Electronics* **2021**, *10*, 1123. [CrossRef]
3. Lu, S.W.; Zhang, S.H.; Chang, H.; Zheng, S.Q.; Song, B. Speed-command-independent parameters self-tuning and mismatch compensation for servo speed control. *Control. Eng. Pract.* **2023**, *137*, 105550. [CrossRef]

4. Dan, F.; He, H.L.; Lu, S.W.; Ma, Y.J. Parallel Self-Tuning Controllers for Speed Servo System Based on Predictive Model-Mismatch Compensation. *IEEE Access* **2024**, *12*, 31968–31976. [CrossRef]
5. Mao, S.; Diao, X.; Ding, L. A non-intervention self-tuning method for PI control parameters in a PMSM servo system with three closed loops. *IEICE Electron. Express* **2025**, *22*, 20250464. [CrossRef]
6. Sabir, M.M.; Ali, T. Optimal PID controller design through swarm intelligence algorithms for sun tracking system. *Appl. Math. Comput.* **2016**, *274*, 690–699. [CrossRef]
7. Yang, F.; Su, X.; Ren, X. Optimization of Active Disturbance Rejection Control System for Vehicle Servo Platform Based on Artificial Intelligence Algorithm. *Electronics* **2025**, *14*, 752. [CrossRef]
8. Hsieh, Y.Z.; Lin, S.S. Robotic Arm Assistance System Based on Simple Stereo Matching and Q-Learning Optimization. *IEEE Sens. J.* **2020**, *20*, 10945–10954. [CrossRef]
9. Xin, W.; Ran, L.; Yanghua, W.; Yong, P.; Bin, Q. Self-tuning PID Controller with Variable Parameters Based on Particle Swarm Optimization. In Proceedings of the 2013 Third International Conference on Intelligent System Design and Engineering Applications, Hong Kong, 16–18 January 2013; pp. 1264–1267.
10. Tao, X.; Liu, K.; Yang, J.; Chen, Y.; Chen, J.; Zhu, H. Sliding Mode Backstepping Control of Excavator Bucket Trajectory Synovial in Particle Swarm Optimization Algorithm and Neural Network Disturbance Observer. *Actuators* **2025**, *14*, 9. [CrossRef]
11. Fang, S.; Wang, Y.; Wang, W.; Chen, Y.; Chen, Y. Design of Permanent Magnet Synchronous Motor Servo System Based on Improved Particle Swarm Optimization. *IEEE Trans. Power Electron.* **2022**, *37*, 5833–5846. [CrossRef]
12. Zhong, X.; Tao, W.; Zou, L.; Yang, H.; Yao, S. Servo System Control of Turntable Lipstick-Filling Machine Based on Particle Swarm Optimization. *Adv. Mater. Sci. Eng.* **2022**, *2022*, 8968510. [CrossRef]
13. Mu, S.; Shibata, S.; Baba, D.; Oshita, R. A Study on a Variable-Gain PID Control for a Pneumatic Servo System Using an Optimized PSO-Type Neural Network. *Actuators* **2025**, *14*, 250. [CrossRef]
14. Gyimah, N.; Jõemaa, R.; Pärnamets, K.; Scheler, O.; Rang, T.; Pardy, T. PID Controller Tuning Optimization Using Genetic Algorithm for Droplet Size Control in Microfluidics. In Proceedings of the 2022 18th Biennial Baltic Electronics Conference (BEC), Tallinn, Estonia, 4–6 October 2022; pp. 1–6.
15. Liu, H.; He, Y.; He, J. Research on Incremental Adaptive Fuzzy PID Algorithm for Permanent Magnet Synchronous Motor System. In Proceedings of the 2022 23rd International Conference on Electronic Packaging Technology (ICEPT), Dalian, China, 10–13 August 2022; pp. 1–5.
16. Guo, Y.-Q.; Zha, X.-M.; Shen, Y.-Y.; Wang, Y.-N.; Chen, G. Research on PID Position Control of a Hydraulic Servo System Based on Kalman Genetic Optimization. *Actuators* **2022**, *11*, 162. [CrossRef]
17. Cao, F. PID controller optimized by genetic algorithm for direct-drive servo system. *Neural Comput. Appl.* **2020**, *32*, 23–30. [CrossRef]
18. Mingxue, L.; Guolai, Y.; Xiaoqing, L.; Guixiang, B. Variable Universe Fuzzy Control of Adjustable Hydraulic Torque Converter Based on Multi-Population Genetic Algorithm. *IEEE Access* **2019**, *7*, 29236–29244. [CrossRef]
19. Mirjalili, S.; Lewis, A. The Whale Optimization Algorithm. *Adv. Eng. Softw.* **2016**, *95*, 51–67. [CrossRef]
20. Srivastava, A.; Das, D.K.; Rai, A.; Raj, R. Parameter Estimation of a Permanent Magnet Synchronous Motor using Whale Optimization Algorithm. In Proceedings of the 2018 Recent Advances on Engineering, Technology and Computational Sciences (RAETCS), Allahabad, India, 6–8 February 2018; pp. 1–6.
21. Khaniki, M.A.L.; Esfandiari, S.; Manthouri, M. Speed Control of Brushless DC motor using Fractional Order Fuzzy PI Controller Optimized via WOA. In Proceedings of the 2020 10th International Conference on Computer and Knowledge Engineering (ICCKE), Mashhad, Iran, 29–30 October 2020; pp. 431–436.
22. Choi, A.; Ahn, H.; Chung, Y.; You, K. Sliding Mode Control for Sensorless Speed Tracking of PMSM with Whale Optimization Algorithm and Extended Kalman Filter. *Machines* **2023**, *11*, 851. [CrossRef]
23. Feng, W.; Deng, B. Global convergence analysis and research on parameter selection of whale optimization algorithm. *Control. Theory Appl.* **2021**, *38*, 641–651.

Disclaimer/Publisher's Note: The statements, opinions and data contained in all publications are solely those of the individual author(s) and contributor(s) and not of MDPI and/or the editor(s). MDPI and/or the editor(s) disclaim responsibility for any injury to people or property resulting from any ideas, methods, instructions or products referred to in the content.